Powder Metallurgy Progress, Vol.18 (2018), No.1, p.006-020
http://dx.doi.org/10.1515/pmp-2018-0002

THE ROLE OF THE ATMOSPHERE ON BORON-ACTIVATED SINTERING OF FERROUS POWDER COMPACTS

V. Vassileva, H. Danninger, S. Strobl, Ch. Gierl-Mayer, R. de Oro Calderon, H. Hutter

Abstract

Boron has been known to activate densification during sintering of ferrous powder compacts, though with risk of embrittlement. In the present study, specimens Fe-B and Fe-C-B prepared from standard atomized iron powder with addition of ferroboron Fe-21%B were sintered in different atmospheres, and the resulting microstructures and properties were studied. It showed that the activating effect of boron is observed during sintering in argon and in hydrogen while sintering in N_2 containing atmospheres results in rapid deactivation of boron, through formation of stable BN. In hydrogen atmosphere, surface deboronizing was observed to considerable depth. Ar is chemically inert, but Ar trapped inside closed pores tends to inhibit further densification. The impact energy data indicated that the embrittling effect of boron is enhanced significantly by presence of carbon. In the fracture surfaces, transgranular cleavage fracture can be observed both at very low and high impact energy values.

Keywords: Sintered steels, boron, atmosphere, embrittlement

INTRODUCTION

For sintered steels, the density is the single factor that dominates the properties, especially the mechanical ones. High sintered density is therefore a most attractive target, and in addition to compacting techniques, also activating the sintering process is a viable way to increase the sintered density level, at least if shrinkage occurs in a stable way and distortion is avoided. One of the most effective sintering activators is boron, as has been shown already in the 1950s [1]. Boron is virtually insoluble in iron or steel, and it forms a eutectic melt above about 1170°C [2]. In ferrous powder compacts, persistent liquid phase is generated in this temperature range that strongly promotes densification [3].

This effect has been used for sintering of numerous types of PM steels [4-6], also different boron carriers being employed such as elemental boron, ferroboron, or B containing masteralloys [7, 8]. Also hexagonal boron nitride has been used which decomposes in N-free atmospheres [9-11], forming Fe-B liquid phase. On the other hand, however, the very low solubility of B both in austenite and ferrite means that the persistent liquid phase solidifies in situ, and above a given B content a continuous network of boride eutectic remains that results in pronounced embrittlement of the sintered compact, at least in mechanical properties that are significantly inferior to those that could be expected from the density level.

Vassilka Vassileva*, Herbert Danninger, Susanne Strobl, Christian Gierl-Mayer, Raquel de Oro Calderon, Herbert Hutter: Technische Universität Wien, Institut für Chemische Technologien und Analytik, Getreidemarkt 9/164, A-1060 Wien/Vienna, Austria, *now: OMV AG, A-1020 Wien/Vienna, Austria

In [9] it has been shown that for gravity sintered, highly porous stainless steel filters the presence of eutectic boride layers at the sintering contacts is not a problem as long as these eutectic regions are isolated since they are sufficiently strong that during mechanical loading the plastic deformation is shifted to the ductile austenitic base material. If however the eutectic structure is interconnected, i.e. continuous, – and if the matrix itself is only moderately ductile – failure in one location will result in immediate brittle failure along the boride structure. The success of boride activation therefore depends on the concentration of boron available: it has to be chosen at such a level that is sufficiently high to yield the desired activation, i.e. densification; on the other hand it should be sufficiently low that only local boride eutectic remains and formation of interconnected areas is precluded. This "concentration window" is reportedly rather narrow, and it can be assumed that it is also defined by the presence of alloy elements such as carbon or Mo [12, 13]. Also other elements such as Ni [8] or Mn [14] have been shown to affect the microstructure and thus the mechanical properties. Furthermore, boron is known to react with constituents of the sintering atmosphere such as hydrogen to form volatile compounds [15, 16], and it is also a strong nitride former. As stated above, hexagonal boron nitride admixed to steel powder has been shown to decompose during sintering e.g. in vacuum, resulting in boron activation, but on the other hand also the reverse reaction, i.e. reaction of boron with N_2 from the atmosphere, with subsequent formation of inert hBN, can be expected, as has been shown e.g. by Momeni [10].

In this work, the sintering behaviour of ferrous compacts containing varying amounts of boron was studied in different atmospheres, both plain Fe and Fe-C matrices being employed.

EXPERIMENTAL TECHNIQUE

The base powder used was plain iron powder ASC 100.29 (Höganäs AB); in part natural graphite UF4 (Kropfmuehl) was admixed. Boron was introduced as ferroboron powder (Fe-21 mass%B) supplied by IMR Kosice. This powder was mostly fine (<45 µm) but contained some coarser fractions that were not screened off but were retained as markers for liquid phase formation, coarse secondary pores indicating that liquid phase has been generated during sintering (see below), which however did not affect the distribution of the liquid phase 0.5 mass% EBS (Microwax C) was added as pressing lubricant. The powders were dry blended for 60 min in a tumbling mixer and uniaxially compacted in a tool with floating die to standard impact test bars (ISO 5754) 55 x 10 x ca. 8 mm^3. The compacting pressure was uniformly 600 MPa. Dewaxing was performed separately prior to sintering in a tube furnace in flowing N_2 of 99.999% purity (5.0 grade) for 30 min at 600°C. Sintering in high purity (5.0 grade) N_2 and Ar, respectively, was done in a pushtype furnace heated by SiC rods that was equipped with a gas tight Kanthal APM superalloy muffle, consistently high purity of the atmosphere being thus established. Sintering in H_2 was done in a pusher furnace Degussa "Baby" with Mo heating elements; here sintering of the carbon-containing specimens was done in getter boxes using Al_2O_3 - 5% graphite as getter. In part sintering was performed in parallel at 1200°C and 1300°C, respectively, to study the effect of the varying liquid phase content. Isothermal sintering time was uniformly 60 min. Cooling was done by pushing the boats / getter boxes into the water-jacketed exit zones of the furnaces.

Characterization of the specimens was done following standard techniques: The green density was determined from the mass and dimensions while the sintered density was measured through water displacement; here, the specimens were impregnated before measurement using a commercial waterstop spray, to avoid intrusion of water into open

pores. Mechanical testing included Vickers hardness and Charpy impact energy on unnotched samples, since it has been found that hardness and impact energy are markedly better suited to describe the mechanical behaviour of sintered steels than the usual combination of R_m and A, in particular at low to moderate ductility levels. In all cases, metallographic investigations were performed, 2% Nital (MeOH-2%HNO_3) being used as etchant. The boron distribution was studied in metallographic sections by secondary ion mass spectrometry (SIMS CAMECA 3f, primary ions Cs^+ at 15.5 keV energy, 150 nA current).

RESULTS

Results obtained with Fe-B materials

In Figure 1 the properties obtained when sintering Fe-x%B in flowing high purity argon are shown. Ar was used here since it can be regarded as a chemically inert atmosphere. As can be seen in Fig.1, the green density slightly drops with increasing B content – due to the adverse effect of the admixed hard ferroboron on the compressibility – while the sintered density increases significantly as a consequence of B addition. Sintering at 1300°C is more effective than at 1200°C, but this holds – not surprisingly - also for the reference materials without B. Typically the density increases as a function of the B content only up to about 0.15 to 0.20% and then levels off, in particular when sintering at 1300°C. This effect can be attributed to trapping of the argon in the pores: since Ar is completely insoluble in iron even at high temperatures, pores filled with Ar remain so when the pore morphology changes from open to closed one, and if the pore shrinks due to capillary forces, the internal pressure increases, opposing further densification. This "argon trapping" effect is the reason why materials routinely to be sintered to full density – heavy alloys, hardmetals, tool steels – are never sintered in argon.

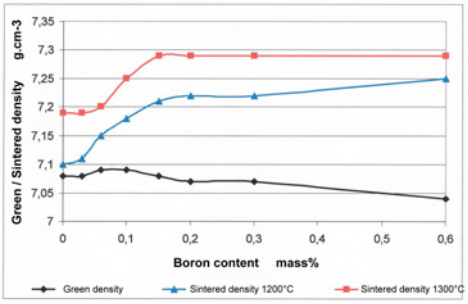

a) Density of Fe-x%B

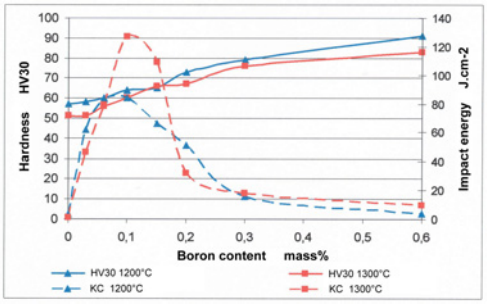

b) Hardness and impact energy

Fig.1. Properties of Fe-x%B sintered in Ar 99.999 as a function of the B content. Fe-21B, compacted at 600 MPa, sintered 60 min isothermal.

When observing the mechanical properties it can be stated that the hardness increases consistently with increasing B content while for the impact energy typical "windows" of optimum B content are discernible, as could be expected from the facts described above. The window is slightly narrower for 1300°C sintering temperature than for 1200°C, indicating that at 1300°C the critical liquid phase content – that results in continuous boride networks after sintering – is obtained at lower B contents than at 1200°C. Nevertheless, the impact energy values obtained are quite impressive - >100 $J.cm^{-2}$ for

0.10% and 0.15%B when sintering at 1300°C – which indicates that here the desired sintering effect has really been obtained without embrittlement.

The extremely low impact energy values obtained for the plain iron reference materials seem to be surprising at first. However, it has to be kept in mind that high purity plain iron tends to exhibit excessive grain growth during the austenite-ferrite transformation [17], which effect is particularly pronounced with sintered plain iron [17-19]. As shown e.g. in [18, 20], those extremely coarse-grained specimens are prone to brittle intergranular fracture, with impact energy values < 5 J.

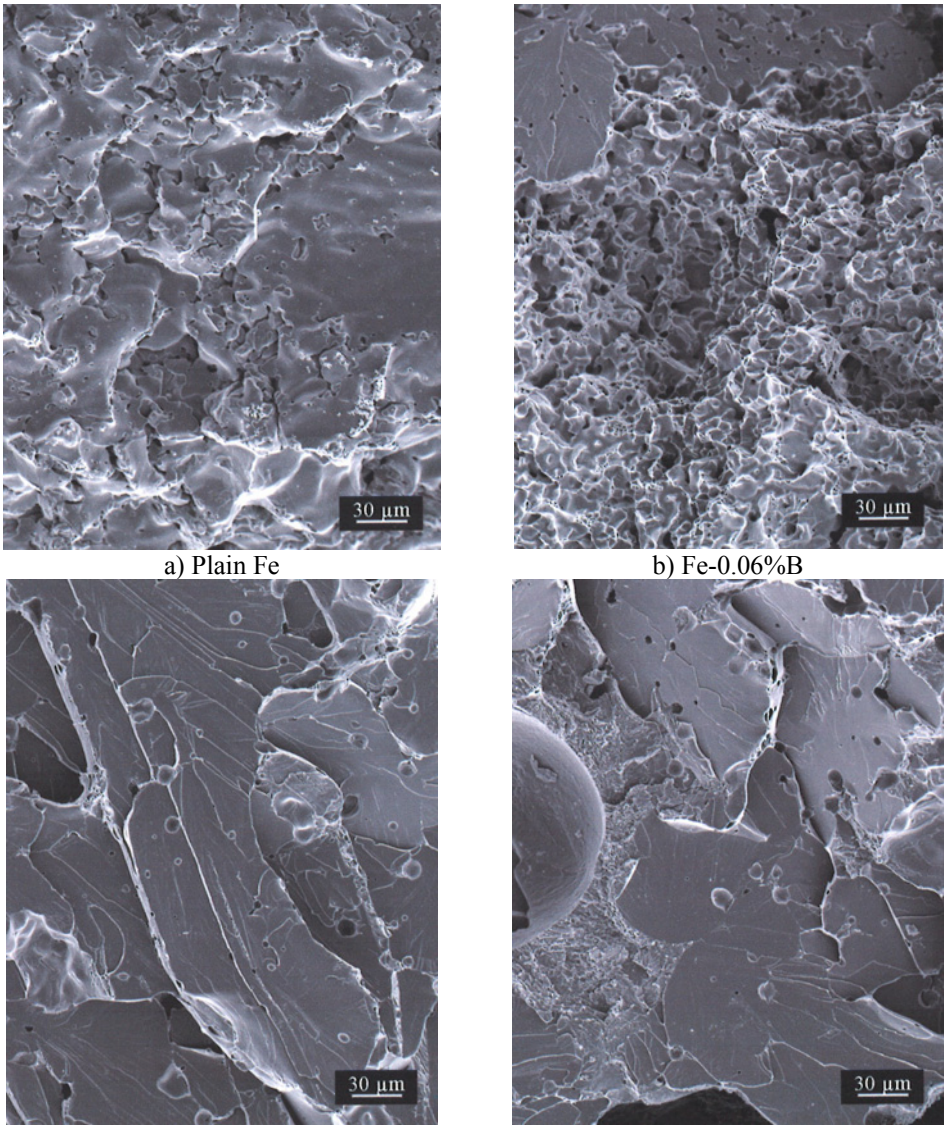

a) Plain Fe b) Fe-0.06%B

c) Fe-0.15%B d) Fe-0.30%B

Fig.2. Fracture surfaces of Fe-x%B, sintered 60 min at 1300°C in Ar. Ferroboron Fe-21B.

The effect can clearly be seen in the fracture surfaces. In figure 2, typical impact fracture surfaces are shown. Here, for the plain iron specimen the typical smooth surface of the intergranular failure can be seen (Fig.2a). At moderate B levels <0.15%B the grain coarsening is already suppressed, and mostly ductile rupture is obtained, localized cleavage being discernible (Fig.2b). This effect of interstitials has also been observed with H, C and N; in the present case also B_2O_3 traces might slow down grain growth, although the fairly high vapour pressure of this oxide renders marked effects rather improbable. Surprisingly, the high impact energy specimens Fe-0.15%B and the rather brittle Fe-0.3%B exhibit almost the same fracture mode, in both cases transgranular cleavage being observed (Fig.2c, d). This confirms the fact observed also e.g. with W heavy alloys [21] that the appearance of cleavage facets does not necessarily mean macroscopically brittle failure since there may have been considerable plastic deformation before cleavage occurs. On the other hand, comparison with standard fine grained sintered iron specimens (see e.g. [22,23]) indicates that boron enhances cleavage fracture, suppressing the ductile rupture typical for these materials.

Sintering the same compact grades in H_2 results in markedly different properties (Fig.3). Here, densification is fairly consistent right up to 0.3%B, then the density drops. As metallographic sections have shown, there is some effect of internal gas formation which at high B levels, when the pores are closed in an early stage of sintering, tends to stabilize the pores, although real blistering was not observed.

The relationship hardness-boron content is similar as in the case of Ar, consistently higher hardness being attained with higher boron levels. On the other hand, the impact energy of the plain iron reference specimens is drastically higher than after sintering in Ar, since there is pronouncedly less grain growth, and the level of interfacial oxygen is reduced [18]. Also here there is a positive effect of B on the impact energy that is more pronounced at 1300°C sintering temperature than at 1200°C, and – at first surprisingly – also extends to higher B levels, which disagrees with the results obtained when sintering in Ar.

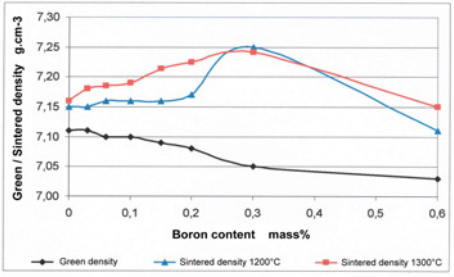

a) Density of Fe-x%B

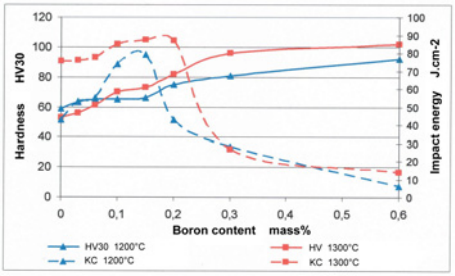

b) Hardness and impact energy

Fig.3. Properties of Fe-x%B sintered in H_2. as a function of the B content. Fe-21B, compacted at 600 MPa, sintered 60 min isothermal.

The reason for this disagreement can at least in part be attributed to the interaction between B and H_2. As was shown by metallographic investigations, there is considerable deboronizing of the specimens in particular at and near the surfaces (Fig.4), clearly indicated by the absence of the characteristic boride network. The deboronized areas are ductile, since there is no embrittling phase; however, ductile areas are found also in the cores at moderate boron levels as visible from the fracture surfaces; compare Fig.5c and Fig.2c, depicting specimens with the same nominal B content. In figure 5c, both cleavage

and pronounced ductile failure stand out clearly. As shown in [16], almost complete deboronizing can be obtained through very long isothermal sintering in hydrogen atmosphere. This results in an almost fully dense and highly ductile material; unfortunately, however, the times necessary render such a process very uneconomical and thus not suitable for industrial practice. In the fracture surfaces also the coarsening of the microstructure caused by persistent iron-boron liquid phase can be seen, which contributes to the loss of ductility at higher B levels.

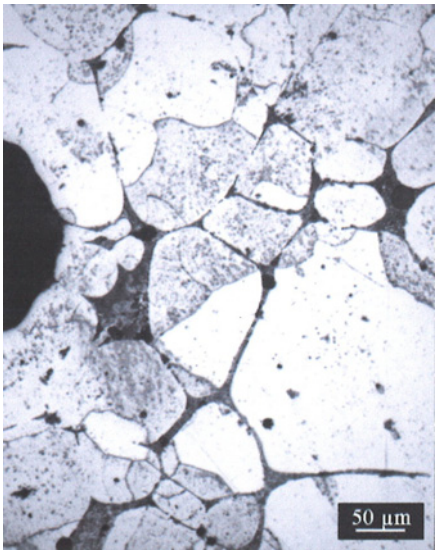

a) Fe-0.3%B

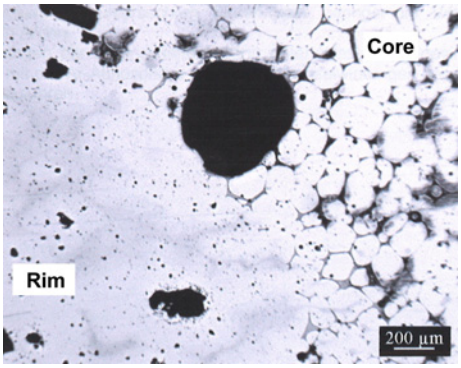

b) Fe-0.6%B, Metallographic section, near surface

Fig.4. Metallographic sections of Fe-x%B, sintered 60 min at 1300°C in H_2.

Sintering in N_2, finally, does no exhibit any signals for B activation: there is neither a significant effect on the density nor on the impact energy – in positive or negative direction. As visible from Fig.6a, the sintered density follows quite the same trend as the green density, simply at a slightly higher level. Hardness and impact energy show a similar behaviour; also there neither the significant enhancement of the impact energy at moderate B contents nor the drop of of this property as a consequence of boride embrittlement is found. This clearly indicates that boron has been deactivated by reaction with the atmosphere. This is also clearly visible from the metallographic section in Fig.7: compared e.g. with Fig.4a the microstructure does not show any traces of liquid phase sintering, and also the coarse ferroboron particles were not dissolved, leaving secondary pores, as shown in Fig.4a, but remained in place, indicating that the boron they contained was no more available to form liquid phase. Also the fracture surfaces resemble those of plain sintered iron (Fig.8).

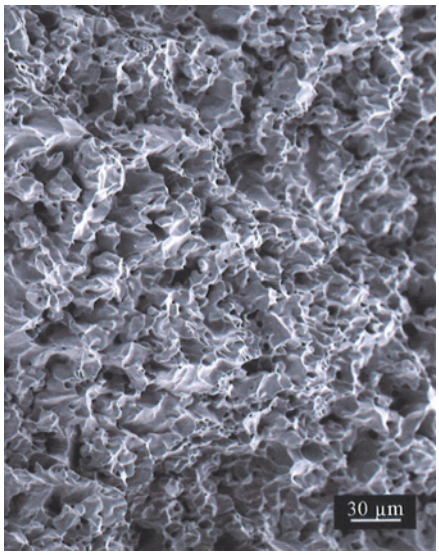

a) plain Fe

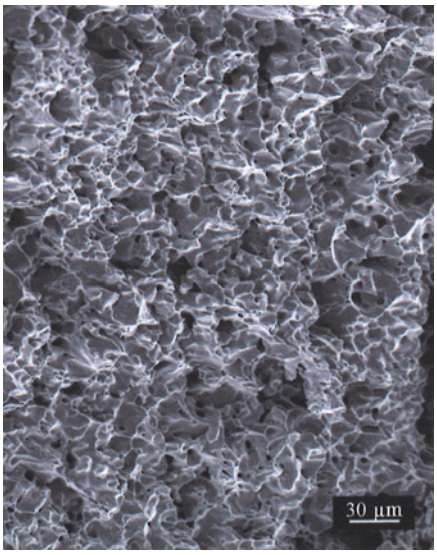

b) Fe-0.06%B

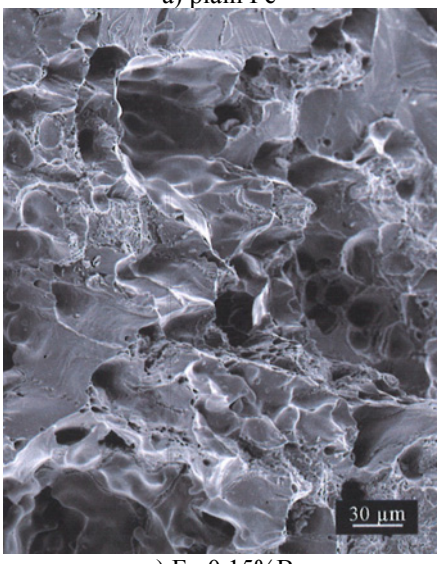

c) Fe-0.15%B

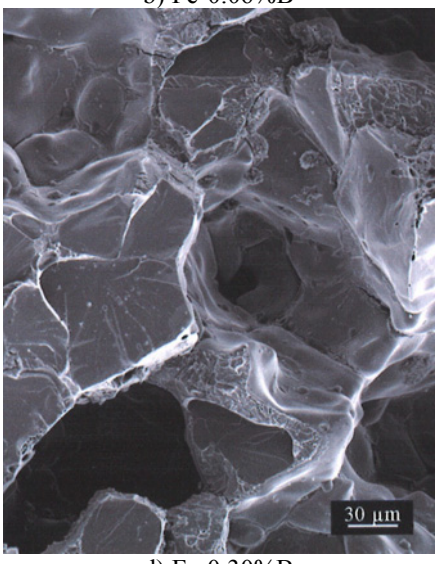

d) Fe-0.30%B

Fig.5. Fracture surfaces of Fe-x%B, sintered 60 min at 1300°C in H_2. Ferroboron Fe-21B.

On metallographic sections, the boron distribution was analyzed through secondary ion mass spectrometry (SIMS). This technique is particularly suited for light elements that are difficult to analyze e.g. by SEM-EDS, boron being particularly tricky. The elemental mappings are shown in Fig.9.

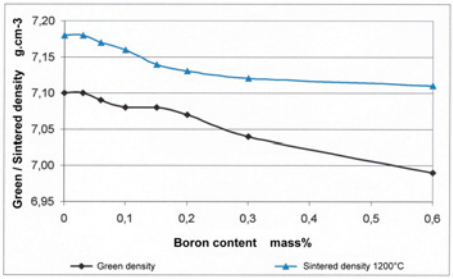

a) Density of Fe-x%B

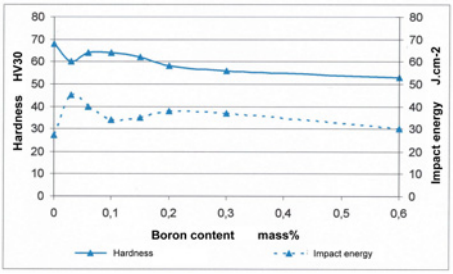

b) Hardness and impact energy

Fig.6. Properties of Fe-x%B sintered in N_2. Fe-21B, compacted at 600 MPa, sintered 60 min isothermal.

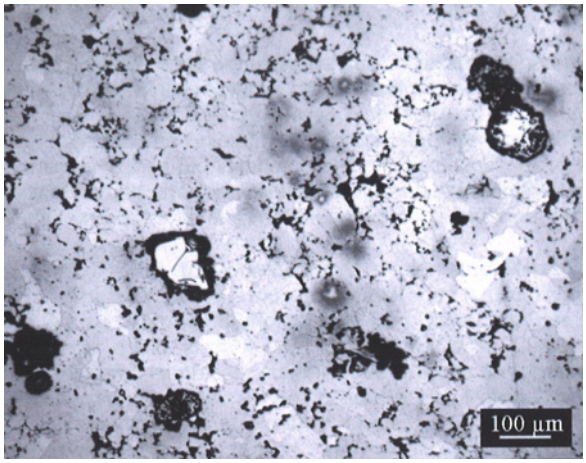

Fig.7. Metallographic section of Fe-0.2%B, sintered 60 min at 1200°C in N_2.

As can be clearly seen, for all boron contents studied the B distribution in specimens sintered in Ar and H_2, respectively, is relatively similar. Evidently the boron phases are isolated at 0.06% and 0.15%B while at 0.30%B continuous networks are visible. This agrees with the impact energy data which show that at 0.15%B fairliy high impact energy is measured while at 0.30%B brittle fracture, with low IE data, are obtained. This once more confirms that the main problem of B activation is the formation of interconnected boride networks that embrittle the materials, although, as visible e.g. in Fig.2c, d and 5d, fracture does not occur in the typical intergranular manner known e.g. from P alloyed sintered steels [24]. In the case of sintering in N_2 none such network is observed, which confirms that liquid phase is not formed here since boron is deactivated by BN formation [10] and remains localized at the sites of the original ferroboron particles (Fig.7).

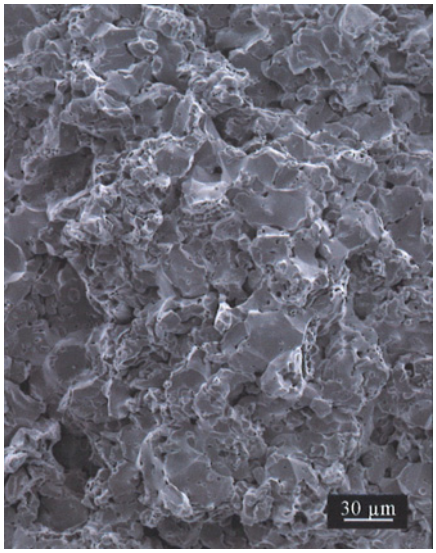

a) 0.00%B

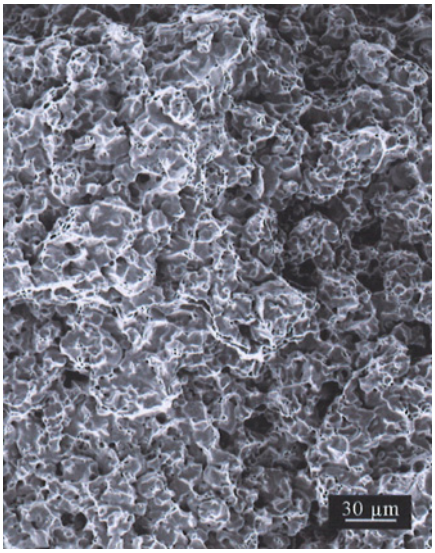

b) 0.06%B

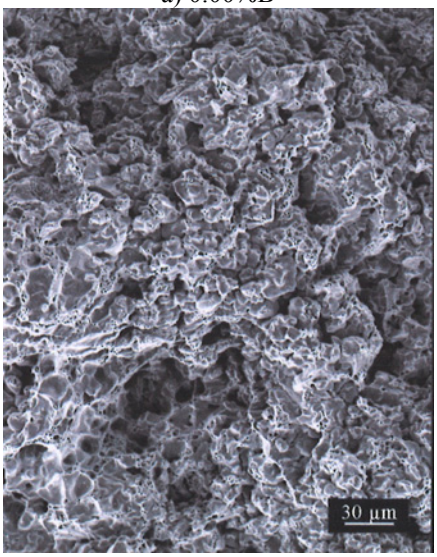

c) 0.15%B

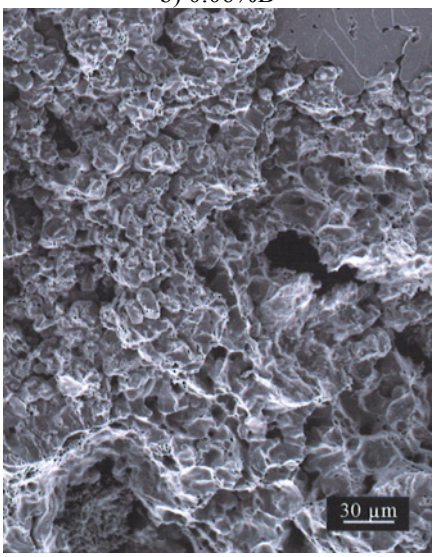

d) 0.30%B

Fig 8. Fracture surfaces of Fe-x%B, sintered 60 min at 1300°C in N_2. Ferroboron Fe-21B.

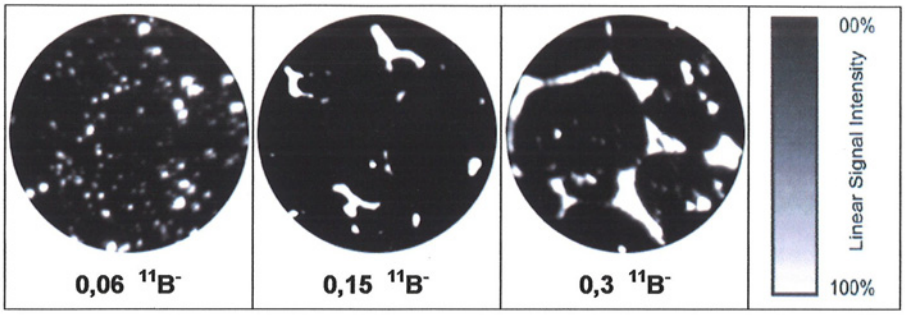

a) Argon

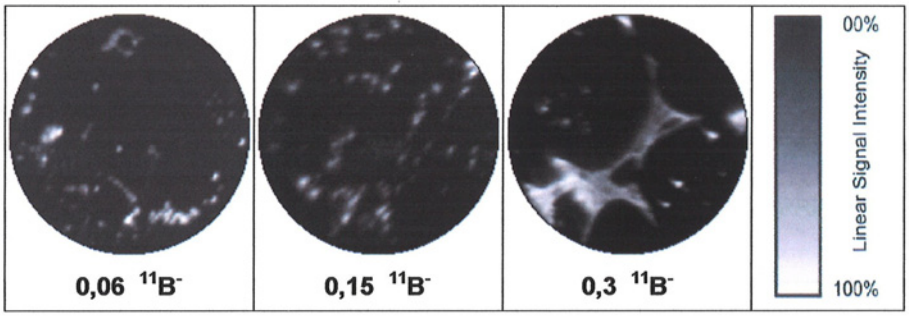

b) Hydrogen

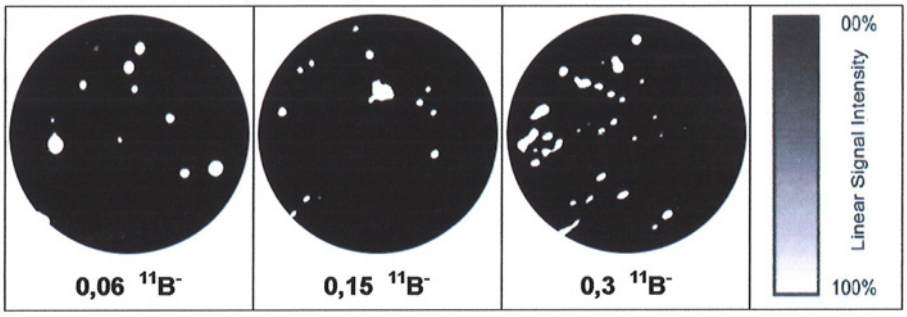

c) Nitrogen

Fig.9. Qualitative SIMS boron mappings of Fe – x%B, compacted at 600 MPa, sintered 60 min 1200°C in different atmospheres (99.999% purity). Image diameter 150 um, Cs^+ ions. Scanned area 300x300 μm^2.

Sintered steels containing boron and carbon

Similar experiments were carried out with materials to which 0.8%C had been admixed as natural graphite. The results obtained by sintering in Ar – as the most inert atmosphere used - are shown in Fig.10.

Here it is evident that apparently the results are basically similar to those obtained without C (see Fig.1) but the trends of the graphs are shifted towards lower B contents. This holds in particular for the impact energy: the drop of the values occurs already at very low

B levels: in fact the Fe-C reference material exhibits the best impact energy, and even when admixing only 0.03%B, the impact energy drops below 10 J.cm^{-2}. Similar effects were observed after sintering in H_2, although here the drop of the impact energy was not quite as pronounced, surely in part as a consequence of the deboronizing effect described above. In any case, the activating effect of boron seems to be still less controllable in carbon containing steels than it is in Fe-B.

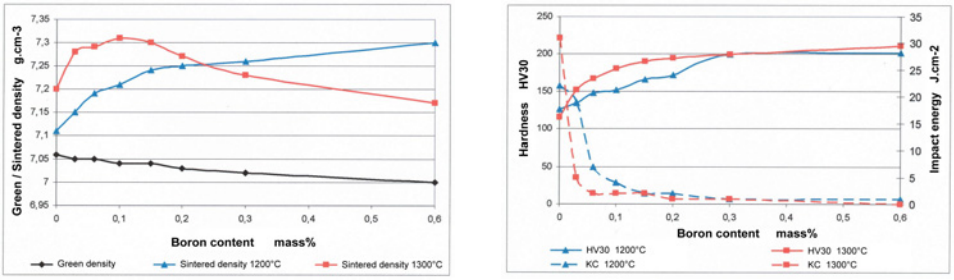

a) Density of Fe-0.8%C-x%B b) Hardness and impact energy

Fig.10. Properties of Fe-0.8%C-x%B sintered in **Ar** as a function of the B content. Fe-21B, compacted at 600 MPa, sintered 60 min isothermal.

When studying the fracture surfaces (Fig.11) it is evident that the tendency to grain coarsening as well as cleavage fracture is more pronounced than with the carbon-free materials; even at as low B contents as 0.06%, coarse microstructure and almost exclusively transgranular fracture are observed (see Fig.11b). Surprisingly, despite the presence of the continuous boride network (see Fig.11d), integranular fracture is not visible even at higher B levels at which the impact energy values are negligible. This disagreement between microstructure and fracture behaviour has to be investigated further.

For those materials sintered in H_2 (Fig.12), a similar trend is observed, although there is a markedly more pronounced effect of the sintering temperature: At 1300°C, at low to moderate B contents markedly more pronounced densification occurs than at 1200°C, but the impact energy drops even at very low boron contents while after sintering at 1200°C, up to 0.15%B acceptable impact energy data are measured, although also here, as in case of sintering in Ar, the best impact energy values are obtained without any B addition. This once more confirms that the combination of C and B has to be handled with extreme care to obtain acceptable mechanical properties. Furthermore, the coincidence between density and impact energy stands out clearly, indicating that densification by itself is not as relevant as is the strengthening of the individual sintering contacts [25].

In case of Fe-C-B, the deboronlizing effect of the H_2 atmosphere stands out very clearly also in the etched section: as shown in Fig.13, there is a clear difference between the core and the rim areas. The former is significantly coarser, as a consequence of the boron activation, while in the near-surface region, to a depth of about 500 um, a fine microstructure as typical for sintered Fe-C can be seen. This indicates that the activating effect of B has not been present here, as a consequence of boron removal through formation of volatile B_2H_6.

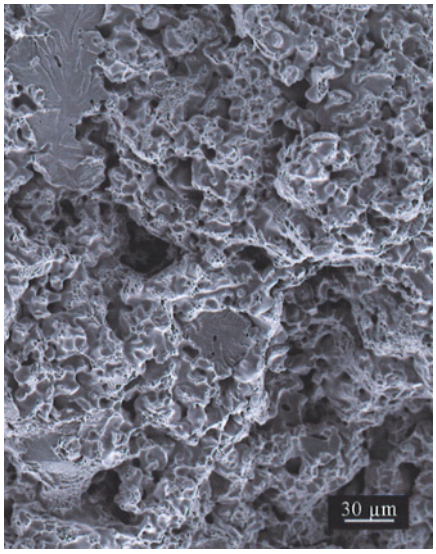

a) Fe-0.8%C

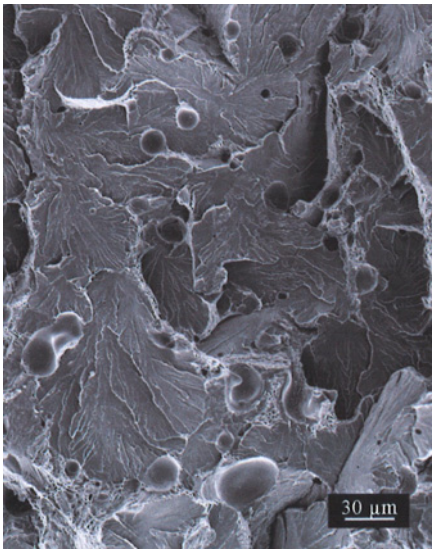

b) Fe-0.8%C-0.06%B

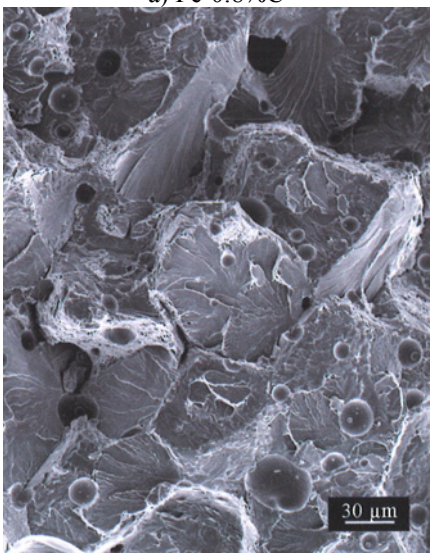

c) Fe-0.8%C-0.3%B

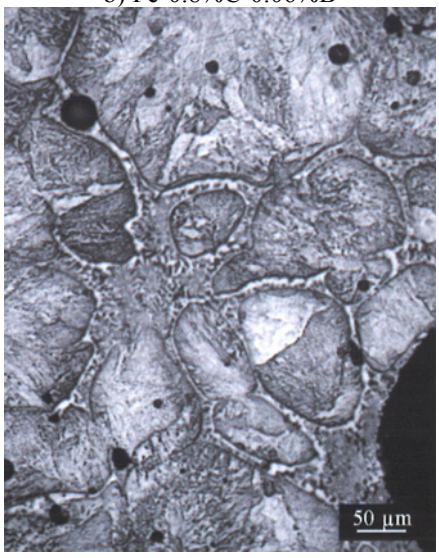

d) as Fig.11c; metallographic section

Fig.11. Fracture surfaces of Fe-0.8%C-x%B sintered at 1300°C in Ar.

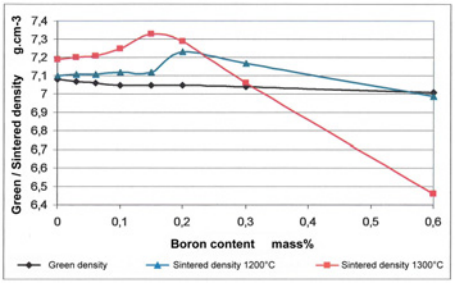

a) Density of Fe-0.8%C-x%B

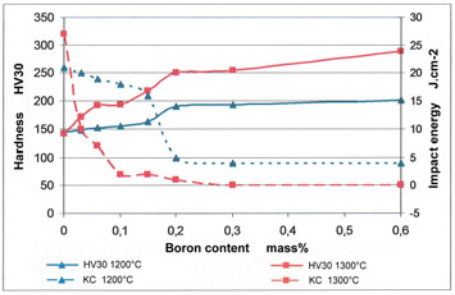

b) HV and impact energy

Fig.12. Properties of Fe-0.8%C-x%B sintered in H_2 as a function of the B content. Fe-21B, compacted at 600 MPa, sintered 60 min isothermal.

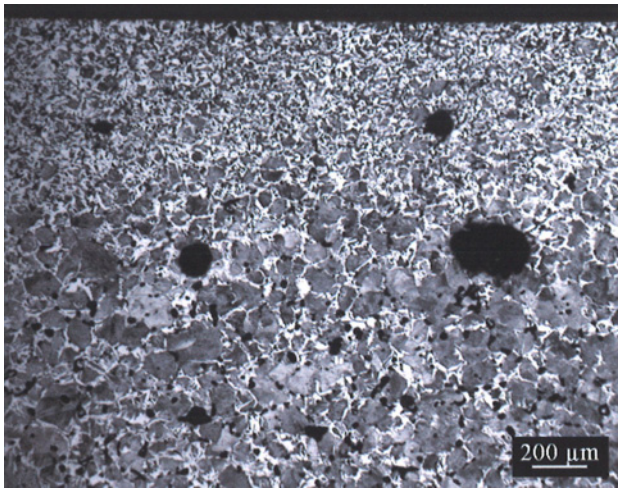

Fig.13. Fe-0.8%C-0.3%B, sintered 60 min at 1300°C in H_2, Nital etched.

The main difference between Fe-B and Fe-C-B is the markedly lower critical B content above which embrittlement occurs. Thermodynamic calculations using the software ThermoCalc were carried out with both systems. They have shown that the combination of B and C in steels results in considerable lowering of the solidus temperature (Fig.14a): this means that on one hand the liquid phase is formed at lower temperature, and on the other hand at a given temperature more liquid phase is formed in case of Fe-B-C than in case of Fe-B, as also indicated in Fig.14b which shows the phase content as a function of the temperature. This can be taken as an indicator that the more severe embrittlement observed with Fe-B-C might be the consequence of the larger volume fraction of liquid phase at the sintering temperatures chosen here and therefore more brittle phase after sintering, the interconnected boride network being formed already at lower B levels than without carbon. In this case, adapting the sintering conditions would be a measure to at least reduce the embrittlement. However, this has to be corroborated by further experimental work, e.g. thermoanalytical studies as well as mechanical testing, and will be the subject of another publication.

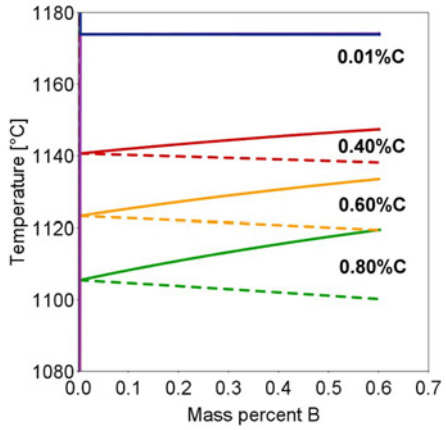

a) Solidus lines in Fe-x%B at different C contents (broken lines: boundary to L+fcc+M2B; solid lines: boundary to L+fcc)

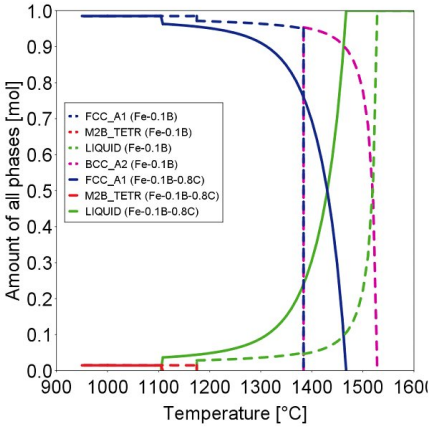

b). Amount of phases in Fe-0.1%B and Fe-0.1%B-0.8%C

Fig.14. Calculated polythermal phase diagrams of Fe-x%B-C.

CONCLUSIONS

In the present study it is shown that sintering of Fe-B with varying B contents in Ar and in H_2 results in the well known activating effect of boron, i.e. in densification and in higher hardness and, at low to moderate B levels, also improved impact energy. At higher B contents the densification effect tends to level off when sintering in Ar, apparently due to the inhibiting effect of Ar trapped in closed pores. The impact energy decreases as a consequence of the formation of brittle boride networks, as clearly visible from SIMS analysis. Surprisingly, even in case of Fe-B materials that show very high impact energy, cleavage fracture dominates, underlining that transgranular cleavage does not necessarily implicate macroscopically brittle behaviour. On the other hand, also the brittle materials fail in a transgranular way and not through plain intergranular fracture as would be expected from a brittle network structure. In H_2, deboronizing occurs, in particular at higher sintering temperatures, resulting in lower B levels than nominal and in less tendency to embrittlement, although the B content thus is still less controllable. Nitrogen deactivates the boron, and the sintering behaviour and properties are similar to those of plain iron.

Addition of 0.8%C increases the tendency to embrittlement. Even B contents <0.1%, which in Fe-B are beneficial, lead to very low impact energy values. In general, the activation of sintering by boron is reasonably controllable in carbon-free materials while in the case of Fe-C-B the “window” for “useful” boron contents – those that are effective towards activation of sintering while still avoiding embrittlement - is narrow and very difficult to control, esp. when regarding the reactivity of B with atmospheric constituents.

Acknowledgement

This work was financially supported by the Austrian Fonds zur Förderung der wissenschaft-lichen Forschung (FWF project no.14889). Furthermore, the assistance and advice of A.Šalak, M.Selecká and E.Dudrová, IMR Kosice, are gratefully acknowledged.

REFERENCES

[1] Benesovsky, F., Hotop, W., Frehn, F.: Planseeberichte Pulvermet., vol. 3, 1955, p. 57
[2] Okamoto, H.: Phase Diagrams of Binary Iron Alloys. Materials Park OH : ASM, 1993
[3] Madan, DS., German, RM., James, WB.: Progress in Powder Metall., vol. 42, 1986, p. 267
[4] Dudrova, E. et al.: Kovove Materialy, vol. 5, 1995, p. 95
[5] Selecká, M., Šalak, A., Danninger, H.: J.Mater.Process.Technol., vol. 143-144, 2003, p. 910
[6] Molinari, A., Straffelini, G., Pieczonka, T., Kazior, J.: Int. J. Powder Metall., vol. 34, 1998, p. 21
[7] Orth, P., Danninger, H., Bouvier, A., Ratzi, R. In: Proc. PM2004 Powder Metallurgy World Congress, Vienna. Eds. H. Danninger, R. Ratzi. Vol. 3. Shrewsbury : EPMA, 2004, p. 307
[8] Gierl-Mayer, C., Zbiral, J., Danninger, H., Ratzi, R. In: Proc. Euro PM2014, Salzburg. Shrewsbury : EPMA, 2014, Paper-Nr. EP14066
[9] Danninger, H., Jangg, G., Giahi, M.: Z.Werkstofftechnik, vol. 19, 1988, p. 205
[10] Momeni, M., Gierl, C., Danninger, H., Avakemian, A.: Powder Metall., vol. 55, 2012, no. 1, p. 54
[11] Momeni, M., Gierl, C., Danninger, H., Ul Mohsin, I., Arvand, A.: Powder Metall., vol. 55, 2012, no. 3, p. 212
[12] Liu, J., Cardamone, A., Potter, TJ., German, RM., Semel, FJ.: Powder Metall., vol. 43, 2000, no. 1, p. 57
[13] Liu, J., German, RM., Cardamone, A., Potter, T., Semel, FJ.: Int. J. Powder Metall., vol. 37, 2001, no. 5, p. 39
[14] Tojal, C., Gomez-Acebo, T., Castro, F.: Mat.Sci.Forum, vol. 534-536, 2007, p. 661
[15] Selecká, M., Bureš, R. In: Proc. Conf. Metallography 1998, IMR Kosice, p. 122
[16] Gierl, C.: PhD thesis. Wien : TU, 1999
[17] Lehr, P.: C.R.Acad.Sci.France, vol. 242, 1956, p. 1172
[18] Danninger, H.: Powder Metall. Progress, vol. 3, 2003, p. 75
[19] Kuroki, H., Suzuki, HY.: Mater. Transactions, vol. 47, 2006, p. 2449
[20] Jaliliziyaeian, M., Gierl, C., Danninger, H. In: Proc. EuroPM2007, Toulouse. Vol. 3. Shrewsbury : EPMA, 2007, p. 131
[21] Danninger, H., Schreiner, M., Jangg , G., Lux, B.: Pract. Metallography, vol. 20, 1983, p. 64
[22] Šlesar, M., Dudrová, E., Parilak, L., Besterci, M., Rudnayová, E.: Sci. Sintering, vol. 19, 1987, p. 17
[23] Danninger, H., Jangg, G., Weiss, B., Stickler, R.: Powder Metall. Int., vol. 25, 1993, no. 4, p. 170; vol. 25, 1993, no. 5, p. 219
[24] Vassileva, V., Krecar, D., Tomastik, C., Gierl-Mayer, C., Hutter, H., Danninger, H.: Powder Metall. Progress, vol. 15, 2015, no. 1, p. 369
[25] Danninger, H., Sonntag, U., Kuhnert, B., Ratzi, R.: Pract.Metallography, vol. 39, 2002, no. 8, p. 414